JACS
JOURNAL OF THE AMERICAN CHEMICAL SOCIETY
pubs.acs.org/JACS
Communication

Using a Function-First "Scout Fragment"-Based Approach to Develop Allosteric Covalent Inhibitors of Conformationally Dynamic Helicase Mechanoenzymes

Jared R. Ramsey, Patrick M. M. Shelton, Tyler K. Heiss, Paul Dominic B. Olinares, Lauren E. Vostal, Heather Soileau, Michael Grasso, Sara W. Casebeer, Stephanie Adaniya, Michael Miller, Shan Sun, David J. Huggins, Robert W. Myers, Brian T. Chait, Ekaterina V. Vinogradova,* and Tarun M. Kapoor*

Cite This: J. Am. Chem. Soc. 2024, 146, 62−67

ABSTRACT: Helicases, classified into six superfamilies, are mechanoenzymes that utilize energy derived from ATP hydrolysis to remodel DNA and RNA substrates. These enzymes have key roles in diverse cellular processes, such as translation, ribosome assembly, and genome maintenance. Helicases with essential functions in certain cancer cells have been identified, and helicases expressed by many viruses are required for their pathogenicity. Therefore, helicases are important targets for chemical probes and therapeutics. However, it has been very challenging to develop chemical inhibitors for helicases, enzymes with high conformational dynamics. We envisioned that electrophilic "scout fragments", which have been used in chemical proteomic studies, could be leveraged to develop covalent inhibitors of helicases. We adopted a function-first approach, combining enzymatic assays with enantiomeric probe pairs and mass spectrometry, to develop a covalent inhibitor that selectively targets an allosteric site in SARS-CoV-2 nsp13, a superfamily-1 helicase. Further, we demonstrate that scout fragments inhibit the activity of two human superfamily-2 helicases, BLM and WRN, involved in genome maintenance. Together, our findings suggest an approach to discover covalent inhibitor starting points and druggable allosteric sites in conformationally dynamic mechanoenzymes.

Developing chemical inhibitors for helicases, which are important targets for antiviral and anticancer drugs, has been notoriously difficult.[1,2] There are at least two reasons why targeting helicases has been challenging. First, while high-throughput activity-based screens have yielded several hits for helicases, the vast majority of these compounds were subsequently found to be nonselective, false positives, or indirect inhibitors (e.g., DNA intercalators).[1] Second, these enzymes undergo substantial conformational changes during their ATP hydrolysis cycle, a property that poses major difficulties for structure-guided inhibitor design.[2] Of the six helicase superfamilies (SFs), the mechanochemical cycles of SF1 and SF2 helicases are well studied.[3] For both helicase superfamilies, two RecA-like domains transition between "open" and "closed" conformations during the ATP hydrolysis cycle,[2] with changes in interdomain spacing reaching ∼15 Å.[4]

We envisioned that a covalent inhibitor discovery approach for helicases could address both challenges, as these compounds would remain bound to the targets throughout the conformational changes linked to the enzymatic cycle (Figure 1A), and direct target engagement could be readily assessed using mass spectrometry (MS) techniques. The use of covalent probes to discover and target allosteric sites has been shown to be an effective strategy for other protein superfamilies that have been difficult to selectively inhibit,[5,6] such as Ras GTPases.[7]

Our efforts were inspired by the use of electrophilic "scout fragments" in large-scale chemical proteomic workflows profiling ligandability across native proteomes.[8−11] Importantly, these chemical proteomic analyses have identified ligandable sites in helicases.[10,11] However, it is unclear whether any of these liganding events inhibit helicase activity and whether these fragments can be progressed into site-specific inhibitors. We also noted that methods to assess if ligand engagement modulates protein function are now emerging.[12,13]

Here, we combine the use of electrophilic "scout fragments" with biochemical assays, enantiomeric probe pairs,[14] and mass spectrometry to identify starting points for inhibitors and targetable allosteric sites in helicases. To develop our approach, we first focused on the SARS-CoV-2 helicase nsp13, a member of the SF1 helicases that is required for SARS-CoV-2 replication.[15,16] Nsp13 has been proposed to be an important target of antiviral therapies due to the high degree of conservation across coronaviruses of potentially druggable pockets in this enzyme.[17] Nsp13 contains five domains (Figure 1B) and can unwind DNA or RNA substrates.[18−20] Efforts to identify inhibitors of nsp13 using crystallographic fragment screens have been reported, but it is unclear if the fragments inhibit helicase function.[19] In addition, target specificity has

Received: September 25, 2023
Revised: December 14, 2023
Accepted: December 15, 2023
Published: December 22, 2023

https://doi.org/10.1021/jacs.3c10581
J. Am. Chem. Soc. 2024, 146, 62−67

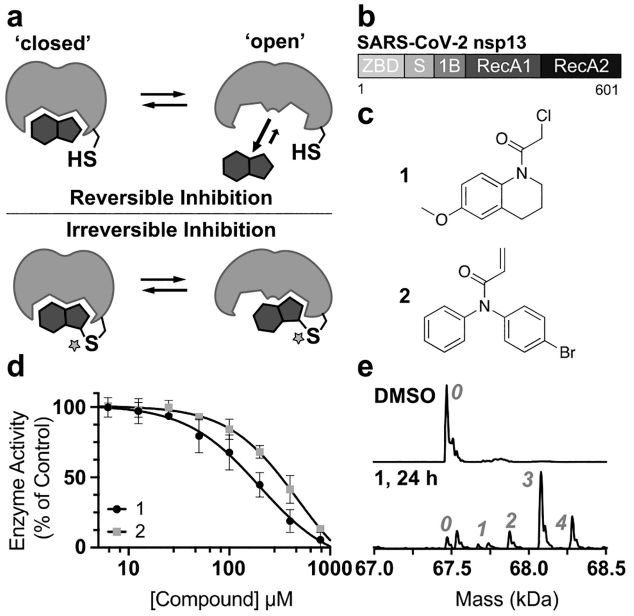

Figure 1. A "scout fragment"-based function-first approach to discover covalent inhibitors of helicases. (a) Schematic of irreversible versus reversible inhibition. (b) Domain organization of nsp13. ZBD: zinc-binding domain; S: stalk; 1B: β-barrel domain. (c) Chemical structure of "scout fragments", **1** (KB02) and **2** (KB05). (d) Dose-dependent inhibition of nsp13 helicase activity by **1** and **2** (IC_{50}: **1** = 198 ± 60 μM, **2** = 357 ± 139 μM; 8 h incubation; 4 °C). (e) nMS analysis of nsp13 liganding by **1** (200 μM, 4 °C; number of adducts: gray).

not been firmly established for inhibitors from high-throughput screening and drug repurposing efforts.[21−23]

To identify covalent inhibitors for nsp13, we selected two previously characterized "scout fragments" (compounds **1** and **2**; Figure 1C).[8−11] We generated recombinant nsp13, adapted a fluorescence-based helicase assay,[20] and observed dose-dependent inhibition of nsp13 by compounds **1** and **2** (Figure 1D). We selected the more potent compound **1** for subsequent studies.

High-resolution native mass spectrometry (nMS) revealed predominantly three covalent adducts on nsp13 in the presence of compound **1** (Figure 1E). Nsp13 contains 26 cysteine residues,[24] and these data indicate that only a subset are liganded by compound **1**. Site-mapping MS indicated that compound **1** modifies C441 and C444, residues in a loop within nsp13's ATP-binding pocket (Figure S1, Table S1). We next generated a construct with two mutations (C441S and C444S, hereafter $nsp13^{C441S\ C444S}$), determined it to be enzymatically active (Figure S2, Table S2), and found that it remained sensitive to compound **1** (Figure S3A).

We performed nMS analysis on $nsp13^{C441S\ C444S}$, and interestingly, only a single adduct was detected after incubation with compound **1** (Figure S3B). This is consistent with the covalent adduction of three cysteine residues (C441, C444, and another) in $nsp13^{wt}$ (Figure 1E). Site-mapping MS experiments indicated that C556 in $nsp13^{C441S\ C444S}$ is the predominant site of modification (Figure S4, Table S3). We next generated a construct with three mutations (C441S C444S C556S), determined it to be enzymatically active (Figure S2 and Table S2), and found that compound **1** does not substantially inhibit its helicase activity (Figure S5).

Encouraged by these data, we synthesized and tested four analogs of compound **1** with simple modifications, such as methyl substitutions (Figure S6). We identified compound **S1**, a racemic mixture that was more potent than compound **1**, and found that its purified enantiomers (compounds **S1a** and **S1b**) display different potencies (Figure S7). Covalent docking studies with **S1b** (Figure S8) guided the synthesis and testing of additional analogs that identified compound **3** (Figure S9). Enantiomers of compound **3** were isolated to obtain compounds **3a** and **3b** (Figure 2A), and again, we observed

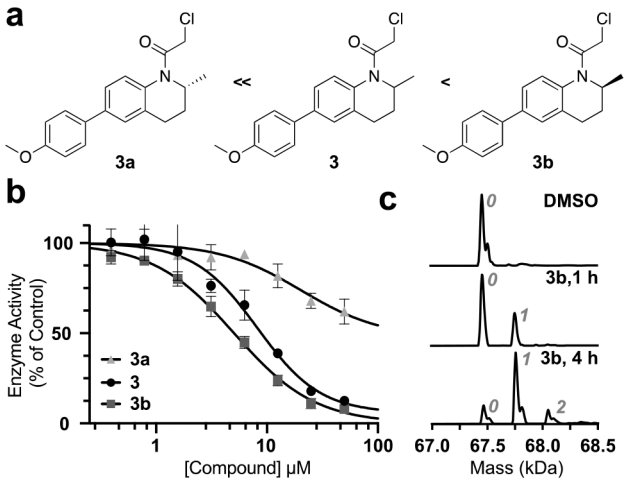

Figure 2. Characterizing analogs of **1**. (a) Chemical structures of **3**, **3a**, and **3b** and potency rank ordering (indicated by chevrons). (b) Dose-dependent inhibition of nsp13 helicase activity by **3**, **3a**, and **3b** (IC_{50}: **3a** > 50 μM; **3** = 8.60 μM ± 0.02; **3b** = 5.04 ± 0.52 μM; 4 h incubation, 4 °C). (c) nMS analysis of $nsp13^{wt}$ liganding by **3b** (20 μM, 4 °C; number of adducts: gray).

differences in the potency of nsp13 inhibition based on the methyl group stereochemistry (Figure 2B). Interestingly, the stereochemistry is different in **3b** relative to **S1b**. Nonetheless, the observed potency differences between **3a** and **3b** suggest that noncovalent contacts play a role in the ligand−enzyme interaction. We also found similar potencies when compound activity was tested at room temperature (Figure S10). nMS analyses indicated that compound **3b**, the more potent enantiomer of compound **3**, liganded nsp13 predominantly at a single residue (Figure 2C).

Site-mapping MS analyses revealed that C556 is the primary site of $nsp13^{wt}$ liganding by compound **3b** (Figure S11, Table S4). We generated a construct with a point mutation at C556 ($nsp13^{C556S}$) determined it to be enzymatically active (Figure S2, Table S2), and gratifyingly, inhibition of this mutant construct by compound **3b** was not detected (Figure 3A). We also performed nMS experiments and did not observe modification of $nsp13^{C556S}$ by compound **3b** (Figure 3B), indicating that **3b** acts by selective covalent modification of the C556 residue in nsp13. We next generated an nsp13 construct with a C556W ($nsp13^{C556W}$) point mutation, as tryptophan mutations can mimic liganding by small molecules.[25] We found that in helicase assays the tryptophan mutant was ~20-fold less active than $nsp13^{wt}$ (Figure 3C). Taken together, these data suggest that covalent modification of C556 suppresses helicase activity.

To profile selectivity, we tested the inhibition of two mammalian helicases by compound **3b**. We selected the

https://doi.org/10.1021/jacs.3c10581
J. Am. Chem. Soc. 2024, 146, 62−67

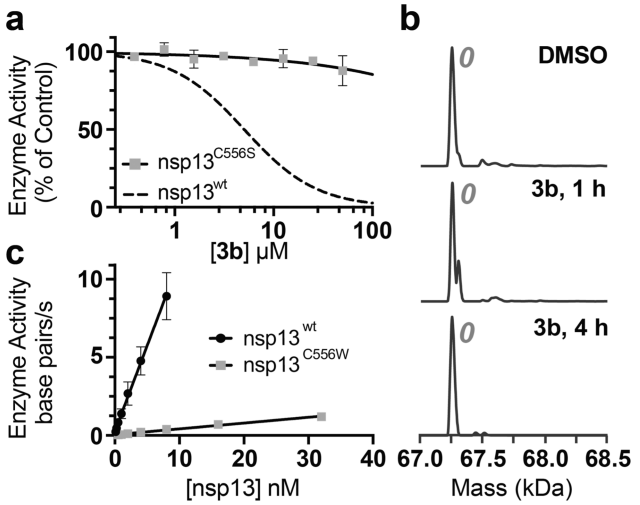

Figure 3. Liganding of C556 leads to nsp13 inhibition. (a) Dose-dependent inhibition of nsp13^{wt} and nsp13^{C556S} by **3b** (data from Figure 2b provided for reference (dashed line); 4 h incubation, 4 °C). (b) nMS analysis of nsp13^{C556S} liganding by **3b** (20 μM, 4 °C; number of adducts: gray). (c) Enzyme velocity versus concentration of nsp13^{wt} and nsp13^{C556W}.

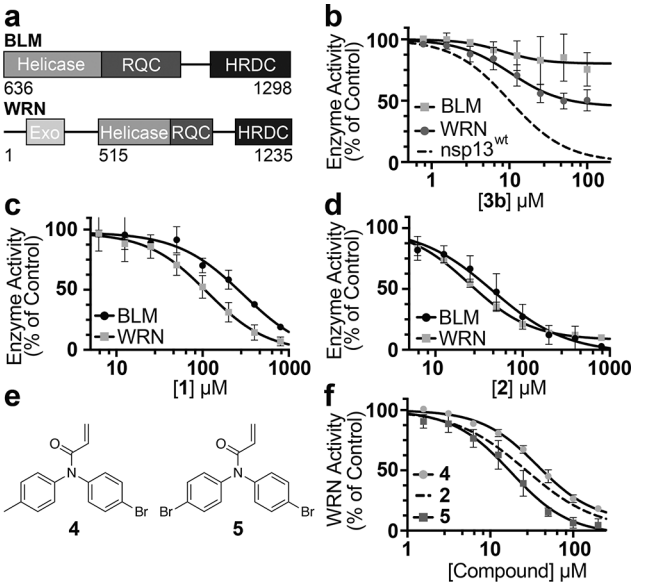

Figure 4. Characterizing inhibition of the helicases BLM and WRN by scout fragments and their analogs. (a) Domain organization of BLM and WRN constructs used. RQC: recQ c-terminal domain; HRDC: helicase and RNAaseD c-terminal domain; Exo: exonuclease domain. (b) Dose-dependent inhibition of nsp13, BLM, and WRN helicase activity by **3b** (IC_{50}: BLM > 100 μM, WRN ~ 50 μM; nsp13: data from Figure 3d provided for reference (dashed line), 4 h incubation, 4 °C). (c) Dose-dependent inhibition of BLM and WRN helicase activity by **1** (IC_{50}: BLM = 243 ± 41 μM; WRN = 114 ± 22 μM; 8 h incubation, 4 °C). (d) Dose-dependent inhibition of BLM and WRN helicase activity by **2** (IC_{50}: BLM = 47.2 ± 20.5 μM; WRN = 24.9 ± 3.8 μM; 8 h incubation, 4 °C). (e) Chemical structures of compounds **4** and **5**. (f) Dose-dependent inhibition of WRN by **4** and **5** (IC_{50}: **4** = 38.3 ± 7.6 μM, **5** = 17.9 ± 6.6 μM; 8 h incubation, 4 °C). Data for **2** from panel d are provided for reference (dashed line).

superfamily-2 RecQ helicases Bloom syndrome (BLM) and Werner syndrome (WRN), enzymes involved in maintaining genome stability.[26] Importantly, WRN helicase has been identified as a unique vulnerability in certain cancer cell lines.[27−30] Guided by literature precedent, constructs for BLM and WRN (BLM$^{636−1298}$, WRN$^{515−1233}$, and WRN$^{1−1235}$ (Figure 4A); generating a near-full-length BLM construct was not successful) were expressed in recombinant form (Figure S12), and fluorescence-based activity assays were adapted.[31,32] We used BLM$^{636−1298}$ and WRN$^{1−1235}$ to profile specificity and found that nsp13 is inhibited by compound **3b** more potently than WRN or BLM (Figure 4B). Together, these data suggest that compound **3b** is a biochemically selective, site-specific, allosteric inhibitor of nsp13.

We next examined if a function-first "scout fragment"-based approach can be used to identify inhibitors of mammalian RecQ helicases. Chemical proteomic studies have suggested that both BLM and WRN can be partially liganded by compounds **1** and **2**.[10,11] For these experiments, we tested scout fragments against BLM$^{636−1298}$ and the equivalent WRN$^{515−1233}$ construct. We found that both BLM and WRN are inhibited by compounds **1** and **2**, but more potently by compound **2** (Figure 4C, 4D). We synthesized and tested two analogs of compound **2**, yielding compounds **4** and **5** (Figure 4E), and found that compound **6** is a more potent inhibitor of WRN than compound **2** (Figure 4F). These data suggest that compounds **2** and **5** could be useful starting points to develop covalent inhibitors for RecQ helicases.

Together, our findings suggest a function-first approach, based on biochemical testing of electrophilic scout fragments combined with the use of enantiomeric probe pairs[14] and mass spectrometry, to identify starting points for inhibitors and druggable allosteric sites in helicase mechanoenzymes. In the case of nsp13, of the 26 cysteines, we identified a single residue in an allosteric site that can be liganded by compound **3b** to inhibit helicase activity. Structural models reveal that C556 is not likely to be directly involved in ATP or RNA binding.[33] Further studies will be required to understand how liganding C556 in nsp13 allosterically inhibits helicase activity. Our finding that nsp13 activity is reduced by mutating this cysteine to serine (Figure S2 and Table S2), a conservative amino acid substitution, suggests that potential inhibitor-resistance-conferring mutations would have an associated fitness cost for the virus. Consistent with this hypothesis, sequences of SARS-CoV-2 in the GISAID database indicate a low frequency of C556 mutations (132 of >15 million sequences available).[34] While electrophilic warheads such as acrylamides are found in clinically approved drugs,[35−37] the chloroacetamide warhead in **3b** is more chemically reactive and likely to have additional cellular targets. Encouragingly, there are examples of chloroacetamide-containing selective probes that have cellular activity.[11] It is noteworthy that less reactive warheads, which retain the overall nucleophilic cysteine attack vector of chloroacetamides, have been developed and could be incorporated in **3b** analogs,[38] as needed.

For the few helicases for which selective chemical inhibitors have been reported,[39−43] targeting allosteric sites has been an effective strategy. In the case of the hepatitis C NS3 helicase, integrative approaches, which included high-throughput screens, fragment screens, and structural analysis, were employed to identify druggable allosteric sites.[39,40] Both allosteric and orthosteric inhibitors of the Brr2 helicase, an enzyme involved in spliceosome function, were identified, and the allosteric binders exhibited better specificity.[41] Characterizing the mechanisms of action of natural products (e.g., rocaglamids) or screening hits has also serendipitously

https://doi.org/10.1021/jacs.3c10581
J. Am. Chem. Soc. 2024, 146, 62−67

identified druggable allosteric sites in EIF4A[42] and BLM helicases,[43] respectively. Our data suggest that characterizing scout fragment-based inhibition may present a useful approach to identify starting points for chemical inhibitors that selectively target allosteric sites in helicases and other conformationally dynamic mechanoenzymes.

■ ASSOCIATED CONTENT

Supporting Information

The Supporting Information is available free of charge at https://pubs.acs.org/doi/10.1021/jacs.3c10581.

Methods, biochemical characterization of nsp13, BLM and WRN constructs, additional nsp13 mutant analyses, site-mapping MS data, analog screens, and computational docking model (PDF)

■ AUTHOR INFORMATION

Corresponding Authors

Ekaterina V. Vinogradova − *Tri-Institutional PhD Program in Chemical Biology, New York, New York 10021, United States; Laboratory of Chemical Immunology and Proteomics, The Rockefeller University, New York, New York 10065, United States*; Email: vinograd@rockefeller.edu

Tarun M. Kapoor − *Laboratory of Chemistry and Cell Biology, The Rockefeller University, New York, New York 10065, United States; Tri-Institutional PhD Program in Chemical Biology, New York, New York 10021, United States*; orcid.org/0000-0003-0628-211X; Email: kapoor@rockefeller.edu

Authors

Jared R. Ramsey − *Tri-Institutional PhD Program in Chemical Biology, New York, New York 10021, United States; Laboratory of Chemistry and Cell Biology, The Rockefeller University, New York, New York 10065, United States*; orcid.org/0000-0002-9536-2164

Patrick M. M. Shelton − *Laboratory of Chemistry and Cell Biology, The Rockefeller University, New York, New York 10065, United States*

Tyler K. Heiss − *Laboratory of Chemistry and Cell Biology, The Rockefeller University, New York, New York 10065, United States*

Paul Dominic B. Olinares − *Laboratory of Mass Spectrometry and Gaseous Ion Chemistry, The Rockefeller University, New York, New York 10065, United States*

Lauren E. Vostal − *Tri-Institutional PhD Program in Chemical Biology, New York, New York 10021, United States; Laboratory of Chemistry and Cell Biology, The Rockefeller University, New York, New York 10065, United States*; orcid.org/0000-0001-9128-7489

Heather Soileau − *Tri-Institutional PhD Program in Chemical Biology, New York, New York 10021, United States; Laboratory of Chemistry and Cell Biology, The Rockefeller University, New York, New York 10065, United States*; orcid.org/0000-0001-7084-8072

Michael Grasso − *Laboratory of Chemistry and Cell Biology, The Rockefeller University, New York, New York 10065, United States*

Sara W. Casebeer − *Laboratory of Chemistry and Cell Biology, The Rockefeller University, New York, New York 10065, United States*

Stephanie Adaniya − *Laboratory of Chemical Immunology and Proteomics, The Rockefeller University, New York, New York 10065, United States*

Michael Miller − *Sanders Tri-Institutional Therapeutics Discovery Institute, New York, New York 10065, United States*

Shan Sun − *Sanders Tri-Institutional Therapeutics Discovery Institute, New York, New York 10065, United States*

David J. Huggins − *Sanders Tri-Institutional Therapeutics Discovery Institute, New York, New York 10065, United States; Department of Physiology and Biophysics, Weill Cornell Medicine, New York, New York 10021, United States*

Robert W. Myers − *Sanders Tri-Institutional Therapeutics Discovery Institute, New York, New York 10065, United States*; orcid.org/0000-0003-2599-1050

Brian T. Chait − *Laboratory of Mass Spectrometry and Gaseous Ion Chemistry, The Rockefeller University, New York, New York 10065, United States*

Complete contact information is available at: https://pubs.acs.org/10.1021/jacs.3c10581

Notes

The authors declare the following competing financial interest(s): T. M. Kapoor is a co-founder of and has an ownership interest in RADD Pharmaceuticals Inc. E. V. Vinogradova is listed as a co-inventor on patents with Vividion Therapeutics.

■ ACKNOWLEDGMENTS

T.M.K. is grateful to the NIH/NIGMS (R35GM130234-01) and the Stavros Niarchos Foundation for funding. E.V.V. is grateful to The Rockefeller University start-up fund, The Robertson Foundation, and the Achelis and Bodman Foundation for funding. E.V.V. is also grateful to the Searle Scholars Program. J.R.R., L.E.V., and H.S. were supported by the Tri-Institutional Ph.D. Program in Chemical Biology and the Rockefeller University Graduate program. L.E.V. and H.S. were also supported by the NIH T32 (GM115327 and GM136640) Chemistry-Biology Interface Training Grant to the Tri-Institutional Ph.D Program in Chemical Biology. B.T.C. is grateful to the NIH for funding (P41 GM109824 and P41 GM103314). Support for this project was also provided by the Sanders Tri-Institutional Therapeutics Discovery Institute (TDI), a 501(c) (3) organization. TDI receives financial support from Takeda Pharmaceutical Company, TDI's parent institutes (Memorial Sloan Kettering Cancer Center, The Rockefeller University, and Weill Cornell Medicine), and from a generous contribution from Lewis Sanders and other philanthropic sources. We thank Caroline Webster for assistance with site-mapping MS experiments.

■ REFERENCES

(1) Shadrick, W. R.; Ndjomou, J.; Kolli, R.; Mukherjee, S.; Hanson, A. M.; Frick, D. N. Discovering New Medicines Targeting Helicases: Challenges and Recent Progress. *SLAS Discov* **2013**, *18* (7), 761−781.

(2) Kwong, A. D.; Rao, B. G.; Jeang, K.-T. Viral and Cellular RNA Helicases as Antiviral Targets. *Nat. Rev. Drug Discov* **2005**, *4* (10), 845−853.

(3) Pyle, A. M. Translocation and Unwinding Mechanisms of RNA and DNA Helicases. *Annual Review of Biophysics* **2008**, *37* (1), 317−336.

(4) Gu, M.; Rice, C. M. Three Conformational Snapshots of the Hepatitis C Virus NS3 Helicase Reveal a Ratchet Translocation Mechanism. *Proc. Natl. Acad. Sci. U. S. A.* **2010**, *107* (2), 521−528.
(5) Feldman, H. C.; Merlini, E.; Guijas, C.; DeMeester, K. E.; Njomen, E.; Kozina, E. M.; Yokoyama, M.; Vinogradova, E.; Reardon, H. T.; Melillo, B.; Schreiber, S. L.; Loreto, A.; Blankman, J. L.; Cravatt, B. F. Selective Inhibitors of SARM1 Targeting an Allosteric Cysteine in the Autoregulatory ARM Domain. *Proc. Natl. Acad. Sci. U. S. A.* **2022**, *119* (35), No. e2208457119.
(6) Kavanagh, M. E.; Horning, B. D.; Khattri, R.; Roy, N.; Lu, J. P.; Whitby, L. R.; Ye, E.; Brannon, J. C.; Parker, A.; Chick, J. M.; Eissler, C. L.; Wong, A. J.; Rodriguez, J. L.; Rodiles, S.; Masuda, K.; Teijaro, J. R.; Simon, G. M.; Patricelli, M. P.; Cravatt, B. F. Selective Inhibitors of JAK1 Targeting an Isoform-Restricted Allosteric Cysteine. *Nat. Chem. Biol.* **2022**, *18* (12), 1388−1398.
(7) Ostrem, J. M.; Peters, U.; Sos, M. L.; Wells, J. A.; Shokat, K. M. K-Ras(G12C) Inhibitors Allosterically Control GTP Affinity and Effector Interactions. *Nature* **2013**, *503* (7477), 548−551.
(8) Backus, K. M.; Correia, B. E.; Lum, K. M.; Forli, S.; Horning, B. D.; González-Páez, G. E.; Chatterjee, S.; Lanning, B. R.; Teijaro, J. R.; Olson, A. J.; Wolan, D. W.; Cravatt, B. F. Proteome-Wide Covalent Ligand Discovery in Native Biological Systems. *Nature* **2016**, *534* (7608), 570−574.
(9) Bar-Peled, L.; Kemper, E. K.; Suciu, R. M.; Vinogradova, E. V.; Backus, K. M.; Horning, B. D.; Paul, T. A.; Ichu, T.-A.; Svensson, R. U.; Olucha, J.; Chang, M. W.; Kok, B. P.; Zhu, Z.; Ihle, N. T.; Dix, M. M.; Jiang, P.; Hayward, M. M.; Saez, E.; Shaw, R. J.; Cravatt, B. F. Chemical Proteomics Identifies Druggable Vulnerabilities in a Genetically Defined Cancer. *Cell* **2017**, *171* (3), 696−709.
(10) Vinogradova, E. V.; Zhang, X.; Remillard, D.; Lazar, D. C.; Suciu, R. M.; Wang, Y.; Bianco, G.; Yamashita, Y.; Crowley, V. M.; Schafroth, M. A.; Yokoyama, M.; Konrad, D. B.; Lum, K. M.; Simon, G. M.; Kemper, E. K.; Lazear, M. R.; Yin, S.; Blewett, M. M.; Dix, M. M.; Nguyen, N.; Shokhirev, M. N.; Chin, E. N.; Lairson, L. L.; Melillo, B.; Schreiber, S. L.; Forli, S.; Teijaro, J. R.; Cravatt, B. F. An Activity-Guided Map of Electrophile-Cysteine Interactions in Primary Human T Cells. *Cell* **2020**, *182* (4), 1009−1026.
(11) Crowley, V. M.; Thielert, M.; Cravatt, B. F. Functionalized Scout Fragments for Site-Specific Covalent Ligand Discovery and Optimization. *ACS Cent. Sci.* **2021**, *7* (4), 613−623.
(12) Lazear, M. R.; Remsberg, J. R.; Jaeger, M. G.; Rothamel, K.; Her, H.; DeMeester, K. E.; Njomen, E.; Hogg, S. J.; Rahman, J.; Whitby, L. R.; Won, S. J.; Schafroth, M. A.; Ogasawara, D.; Yokoyama, M.; Lindsey, G. L.; Li, H.; Germain, J.; Barbas, S.; Vaughan, J.; Hanigan, T. W.; Vartabedian, V. F.; Reinhardt, C. J.; Dix, M. M.; Koo, S. J.; Heo, I.; Teijaro, J. R.; Simon, G. M.; Ghosh, B.; Abdel-Wahab, O.; Ahn, K.; Saghatelian, A.; Melillo, B.; Schreiber, S. L.; Yeo, G. W.; Cravatt, B. F. Proteomic Discovery of Chemical Probes That Perturb Protein Complexes in Human Cells. *Mol. Cell* **2023**, *83* (10), 1725−1742.
(13) Li, H.; Ma, T.; Remsberg, J. R.; Won, S. J.; DeMeester, K. E.; Njomen, E.; Ogasawara, D.; Zhao, K. T.; Huang, T. P.; Lu, B.; Simon, G. M.; Melillo, B.; Schreiber, S. L.; Lykke-Andersen, J.; Liu, D. R.; Cravatt, B. F. Assigning Functionality to Cysteines by Base Editing of Cancer Dependency Genes. *Nat. Chem. Biol.* **2023**, *19*, 1−11.
(14) Wang, Y.; Dix, M. M.; Bianco, G.; Remsberg, J. R.; Lee, H.-Y.; Kalocsay, M.; Gygi, S. P.; Forli, S.; Vite, G.; Lawrence, R. M.; Parker, C. G.; Cravatt, B. F. Expedited Mapping of the Ligandable Proteome Using Fully Functionalized Enantiomeric Probe Pairs. *Nat. Chem.* **2019**, *11* (12), 1113−1123.
(15) Tanner, J. A.; Watt, R. M.; Chai, Y.-B.; Lu, L.-Y.; Lin, M. C.; Peiris, J. S. M.; Poon, L. L. M.; Kung, H.-F.; Huang, J.-D. The Severe Acute Respiratory Syndrome (SARS) Coronavirus NTPase/Helicase Belongs to a Distinct Class of 5′ to 3′ Viral Helicases. *J. Biol. Chem.* **2003**, *278* (41), 39578−39582.
(16) Subissi, L.; Imbert, I.; Ferron, F.; Collet, A.; Coutard, B.; Decroly, E.; Canard, B. SARS-CoV ORF1b-Encoded Nonstructural Proteins 12−16: Replicative Enzymes as Antiviral Targets. *Antiviral Res.* **2014**, *101*, 122−130.
(17) Yazdani, S.; De Maio, N.; Ding, Y.; Shahani, V.; Goldman, N.; Schapira, M. Genetic Variability of the SARS-CoV-2 Pocketome. *J. Proteome Res.* **2021**, *20* (8), 4212−4215.
(18) Chen, J.; Malone, B.; Llewellyn, E.; Grasso, M.; Shelton, P. M. M.; Olinares, P. D. B.; Maruthi, K.; Eng, E. T.; Vatandaslar, H.; Chait, B. T.; Kapoor, T. M.; Darst, S. A.; Campbell, E. A. Structural Basis for Helicase-Polymerase Coupling in the SARS-CoV-2 Replication-Transcription Complex. *Cell* **2020**, *182* (6), 1560−1573.
(19) Newman, J. A.; Douangamath, A.; Yadzani, S.; Yosaatmadja, Y.; Aimon, A.; Brandão-Neto, J.; Dunnett, L.; Gorrie-stone, T.; Skyner, R.; Fearon, D.; Schapira, M.; von Delft, F.; Gileadi, O. Structure, Mechanism and Crystallographic Fragment Screening of the SARS-CoV-2 NSP13 Helicase. *Nat. Commun.* **2021**, *12* (1), 4848.
(20) Mickolajczyk, K. J.; Shelton, P. M. M.; Grasso, M.; Cao, X.; Warrington, S. E.; Aher, A.; Liu, S.; Kapoor, T. M. Force-Dependent Stimulation of RNA Unwinding by SARS-CoV-2 Nsp13 Helicase. *Biophys. J.* **2021**, *120* (6), 1020−1030.
(21) Zeng, J.; Weissmann, F.; Bertolin, A. P.; Posse, V.; Canal, B.; Ulferts, R.; Wu, M.; Harvey, R.; Hussain, S.; Milligan, J. C.; Roustan, C.; Borg, A.; McCoy, L.; Drury, L. S.; Kjaer, S.; McCauley, J.; Howell, M.; Beale, R.; Diffley, J. F. X. Identifying SARS-CoV-2 Antiviral Compounds by Screening for Small Molecule Inhibitors of Nsp13 Helicase. *Biochem. J.* **2021**, *478* (13), 2405−2423.
(22) White, M. A.; Lin, W.; Cheng, X. Discovery of COVID-19 Inhibitors Targeting the SARS-CoV-2 Nsp13 Helicase. *J. Phys. Chem. Lett.* **2020**, *11* (21), 9144−9151.
(23) Lu, L.; Peng, Y.; Yao, H.; Wang, Y.; Li, J.; Yang, Y.; Lin, Z. Punicalagin as an Allosteric NSP13 Helicase Inhibitor Potently Suppresses SARS-CoV-2 Replication in Vitro. *Antiviral Res.* **2022**, *206*, No. 105389.
(24) rep - Replicase polyprotein 1ab - Severe acute respiratory syndrome coronavirus 2 (2019-nCoV) | UniProtKB | UniProt. https://www.uniprot.org/uniprotkb/P0DTD1/entry (accessed 2023−09−22).
(25) Taylor, I. R.; Assimon, V. A.; Kuo, S. Y.; Rinaldi, S.; Li, X.; Young, Z. T.; Morra, G.; Green, K.; Nguyen, D.; Shao, H.; Garneau-Tsodikova, S.; Colombo, G.; Gestwicki, J. E. Tryptophan Scanning Mutagenesis as a Way to Mimic the Compound-Bound State and Probe the Selectivity of Allosteric Inhibitors in Cells. *Chem. Sci.* **2020**, *11* (7), 1892−1904.
(26) Croteau, D. L.; Popuri, V.; Opresko, P. L.; Bohr, V. A. Human RecQ Helicases in DNA Repair, Recombination, and Replication. *Annu. Rev. Biochem.* **2014**, *83* (1), 519−552.
(27) Chan, E. M.; Shibue, T.; McFarland, J. M.; Gaeta, B.; Ghandi, M.; Dumont, N.; Gonzalez, A.; McPartlan, J. S.; Li, T.; Zhang, Y.; Liu, J. B.; Lazaro, J.-B.; Gu, P.; Piett, C. G.; Apffel, A.; Ali, S. O.; Deasy, R.; Keskula, P.; Ng, R. W. S.; Roberts, E. A.; Reznichenko, E.; Leung, L.; Alimova, M.; Schenone, M.; Islam, M.; Maruvka, Y. E.; Liu, Y.; Roper, J.; Raghavan, S.; Giannakis, M.; Tseng, Y.-Y.; Nagel, Z. D.; D'Andrea, A.; Root, D. E.; Boehm, J. S.; Getz, G.; Chang, S.; Golub, T. R.; Tsherniak, A.; Vazquez, F.; Bass, A. J. WRN Helicase Is a Synthetic Lethal Target in Microsatellite Unstable Cancers. *Nature* **2019**, *568* (7753), 551−556.
(28) Lieb, S.; Blaha-Ostermann, S.; Kamper, E.; Rippka, J.; Schwarz, C.; Ehrenhöfer-Wölfer, K.; Schlattl, A.; Wernitznig, A.; Lipp, J. J.; Nagasaka, K.; van der Lelij, P.; Bader, G.; Koi, M.; Goel, A.; Neumüller, R. A.; Peters, J.-M.; Kraut, N.; Pearson, M. A.; Petronczki, M.; Wöhrle, S. Werner Syndrome Helicase Is a Selective Vulnerability of Microsatellite Instability-High Tumor Cells. *eLife* **2019**, *8*, No. e43333.
(29) Kategaya, L.; Perumal, S. K.; Hager, J. H.; Belmont, L. D. Werner Syndrome Helicase Is Required for the Survival of Cancer Cells with Microsatellite Instability. *iScience* **2019**, *13*, 488−497.
(30) van Wietmarschen, N.; Sridharan, S.; Nathan, W. J.; Tubbs, A.; Chan, E. M.; Callen, E.; Wu, W.; Belinky, F.; Tripathi, V.; Wong, N.; Foster, K.; Noorbakhsh, J.; Garimella, K.; Cruz-Migoni, A.; Sommers, J. A.; Huang, Y.; Borah, A. A.; Smith, J. T.; Kalfon, J.; Kesten, N.; Fugger, K.; Walker, R. L.; Dolzhenko, E.; Eberle, M. A.; Hayward, B. E.; Usdin, K.; Freudenreich, C. H.; Brosh, R. M.; West, S. C.;

https://doi.org/10.1021/jacs.3c10581
J. Am. Chem. Soc. 2024, 146, 62−67

McHugh, P. J.; Meltzer, P. S.; Bass, A. J.; Nussenzweig, A. Repeat Expansions Confer WRN Dependence in Microsatellite-Unstable Cancers. *Nature* **2020**, *586* (7828), 292−298.
(31) Nguyen, G. H.; Dexheimer, T. S.; Rosenthal, A. S.; Chu, W. K.; Singh, D. K.; Mosedale, G.; Bachrati, C. Z.; Schultz, L.; Sakurai, M.; Savitsky, P.; Abu, M.; McHugh, P. J.; Bohr, V. A.; Harris, C. C.; Jadhav, A.; Gileadi, O.; Maloney, D. J.; Simeonov, A.; Hickson, I. D. A Small Molecule Inhibitor of the BLM Helicase Modulates Chromosome Stability in Human Cells. *Chem. Biol.* **2013**, *20* (1), 55−62.
(32) Newman, J. A.; Savitsky, P.; Allerston, C. K.; Bizard, A. H.; Ozer,·O.; Sarlos, K.; Liu, Y.; Pardon, E.; Steyaert, J.; Hickson, I. D.; Gileadi, O. Crystal Structure of the Bloom's Syndrome Helicase Indicates a Role for the HRDC Domain in Conformational Changes. *Nucleic Acids Res.* **2015**, *43* (10), 5221−5235.
(33) Chen, J.; Wang, Q.; Malone, B.; Llewellyn, E.; Pechersky, Y.; Maruthi, K.; Eng, E. T.; Perry, J. K.; Campbell, E. A.; Shaw, D. E.; Darst, S. A. Ensemble Cryo-EM Reveals Conformational States of the Nsp13 Helicase in the SARS-CoV-2 Helicase Replication−Transcription Complex. *Nat. Struct Mol. Biol.* **2022**, *29* (3), 250−260.
(34) Khare, S.; Gurry, C.; Freitas, L.; Schultz, M. B.; Bach, G.; Diallo, A.; Akite, N.; Ho, J.; Lee, R. T.; Yeo, W.; Maurer-Stroh, S.; et al. GISAID's Role in Pandemic Response. *China CDC Wkly* **2021**, *3* (49), 1049−1051.
(35) Cameron, F.; Sanford, M. Ibrutinib: First Global Approval. *Drugs* **2014**, *74* (2), 263−271.
(36) Greig, S. L. Osimertinib: First Global Approval. *Drugs* **2016**, *76* (2), 263−273.
(37) Blair, H. A. Sotorasib: First Approval. *Drugs* **2021**, *81* (13), 1573−1579.
(38) Reddi, R. N.; Rogel, A.; Gabizon, R.; Rawale, D. G.; Harish, B.; Marom, S.; Tivon, B.; Arbel, Y. S.; Gurwicz, N.; Oren, R.; David, K.; Liu, J.; Duberstein, S.; Itkin, M.; Malitsky, S.; Barr, H.; Katz, B.-Z.; Herishanu, Y.; Shachar, I.; Shulman, Z.; London, N. Sulfamate Acetamides as Self-Immolative Electrophiles for Covalent Ligand-Directed Release Chemistry. *J. Am. Chem. Soc.* **2023**, *145* (6), 3346−3360.
(39) LaPlante, S. R.; Padyana, A. K.; Abeywardane, A.; Bonneau, P.; Cartier, M.; Coulombe, R.; Jakalian, A.; Wildeson-Jones, J.; Li, X.; Liang, S.; McKercher, G.; White, P.; Zhang, Q.; Taylor, S. J. Integrated Strategies for Identifying Leads That Target the NS3 Helicase of the Hepatitis C Virus. *J. Med. Chem.* **2014**, *57* (5), 2074−2090.
(40) Saalau-Bethell, S. M.; Woodhead, A. J.; Chessari, G.; Carr, M. G.; Coyle, J.; Graham, B.; Hiscock, S. D.; Murray, C. W.; Pathuri, P.; Rich, S. J.; Richardson, C. J.; Williams, P. A.; Jhoti, H. Discovery of an Allosteric Mechanism for the Regulation of HCV NS3 Protein Function. *Nat. Chem. Biol.* **2012**, *8* (11), 920−925.
(41) Iwatani-Yoshihara, M.; Ito, M.; Klein, M. G.; Yamamoto, T.; Yonemori, K.; Tanaka, T.; Miwa, M.; Morishita, D.; Endo, S.; Tjhen, R.; Qin, L.; Nakanishi, A.; Maezaki, H.; Kawamoto, T. Discovery of Allosteric Inhibitors Targeting the Spliceosomal RNA Helicase Brr2. *J. Med. Chem.* **2017**, *60* (13), 5759−5771.
(42) Iwasaki, S.; Iwasaki, W.; Takahashi, M.; Sakamoto, A.; Watanabe, C.; Shichino, Y.; Floor, S. N.; Fujiwara, K.; Mito, M.; Dodo, K.; Sodeoka, M.; Imataka, H.; Honma, T.; Fukuzawa, K.; Ito, T.; Ingolia, N. T. The Translation Inhibitor Rocaglamide Targets a Bimolecular Cavity between eIF4A and Polypurine RNA. *Mol. Cell* **2019**, *73* (4), 738−748.
(43) Chen, X.; Ali, Y. I.; Fisher, C. E.; Arribas-Bosacoma, R.; Rajasekaran, M. B.; Williams, G.; Walker, S.; Booth, J. R.; Hudson, J. J.; Roe, S. M.; Pearl, L. H.; Ward, S. E.; Pearl, F. M.; Oliver, A. W. Uncovering an Allosteric Mode of Action for a Selective Inhibitor of Human Bloom Syndrome Protein. *eLife* **2021**, *10*, e65339.

https://doi.org/10.1021/jacs.3c10581
J. Am. Chem. Soc. 2024, 146, 62−67